

Recycling of titanium machining chips by severe plastic deformation consolidation

P. Luo · H. Xie · M. Paladugu · S. Palanisamy ·
M. S. Dargusch · K. Xia

Received: 10 February 2010 / Accepted: 25 March 2010 / Published online: 13 April 2010
© Springer Science+Business Media, LLC 2010

Abstract It has been demonstrated that severe plastic deformation (SPD) can be used to consolidate particles of a wide range of sizes from nano to micro into fully dense bulk material with good mechanical properties. SPD consolidation allows processing to be conducted at much lower temperatures and is therefore suitable for particles with highly metastable structures such as nanocrystalline. It is especially useful in the fabrication of multiphase materials including metal matrix nanocomposites. In this investigation, SPD consolidation was applied to recycle Ti machining chips. In particular, the as-received chips were consolidated by equal channel angular pressing at temperatures between 400 and 600 °C with the application of a back pressure from 50 to 200 MPa. Fully dense bulk Ti with fine grain sizes was produced, possessing strength comparable or higher than that of commercially pure wrought Ti. It is concluded that SPD consolidation is a promising method for recycling and value-adding of Ti chips.

Introduction

Ultrafine and nanostructured materials have been attracting significant amount of research efforts over the recent two decades with their promised unique properties and many

potential applications [1, 2]. Such materials can either be built up from ultrafine and nanostructured particles, or be obtained by refining originally coarse structured bulk materials. With the latter, severe plastic deformation (SPD) is among the most popular [3]. In particular, equal channel angular pressing (ECAP) [4] and high pressure torsion (HPT) [5] are commonly used by many researchers. A third approach combines the bottom-up and top-down ones and bulk nanostructured alloys and composites are produced by consolidating ultrafine or nano particles by SPD [6, 7]. It offers the following advantages. First, SPD forces the particles to be consolidated to deform and thus excellent bonding and full density are readily achieved, eliminating most of the defects associated with the bottom-up approach. Second, nanostructures may be produced using ultrafine or even micro-sized particles, instead of nano-sized particles, and this would reduce cost, handling difficulties and contamination from particle surfaces. Third, SPD allows consolidation to be carried out at temperatures lower than those used in conventional sintering, and thus special structures and compositions, including nanostructures, amorphous phases and high alloy contents obtained in particles produced by highly non-equilibrium processes such as mechanical alloying and rapid solidification, can be preserved during consolidation. Finally and perhaps more importantly, it is most convenient to combine particles of different types and structures to make metal matrix nanocomposites (MMnCs); this enables novel combinations of phases and gives much more freedom to design of microstructures.

Various materials have been consolidated by SPD (see an overview in [6]). Especially, back pressure equal channel angular pressing (BP-ECAP) has turned out to be an effective process. For example, nano Al particles were successfully consolidated by BP-ECAP to result in an

P. Luo · H. Xie · K. Xia (✉)
Department of Mechanical Engineering and Defence Materials
Technology Centre, University of Melbourne, Melbourne,
VIC 3010, Australia
e-mail: k.xia@unimelb.edu.au

M. Paladugu · S. Palanisamy · M. S. Dargusch
School of Mechanical and Mining Engineering and Defence
Materials Technology Centre, University of Queensland,
St Lucia, QLD 4072, Australia

situ nanocomposite of Al and Al_2O_3 [8, 9]. Ti with high interstitial contents was obtained with ultrahigh strength [10]. Al matrix composites containing nano C particles were produced using a combination of mechanical milling and BP-ECAP [11]. The present paper will, however, focus on the application of SPD consolidation in solid-state recycling of machining chips.

Machining is a necessary process in manufacturing, especially in aerospace and automotive industries. In addition to direct costs associated with machining operation, much of the material is wasted in the form of machining chips. For example, as high as 80% of the Ti material may be lost to machining in biomedical and aerospace manufacturing [12]. It is therefore highly desirable to recycle the machining chips. The most straightforward method is to remelt and cast. However, this approach requires higher energy input, and vacuum or other protection is needed for more reactive metals such as Ti and Mg, adding to the expenses and thus making it less attractive. It appears that particle consolidation processes can be adapted for the purpose of solid-state recycling. A number of papers reported solid-state recycling of Mg chips by using hot extrusion [13, 14], mechanical milling and extrusion [15], cyclic extrusion compression [16] or ECAP [17]. However, little has been done in terms of solid-state recycling of Ti machining chips which are of more concerns to the industry. Owing to its high reactivity, SPD-based consolidation processes are perhaps most suitable for Ti since lower processing temperatures can be used. To be able to handle the expected large volume, ECAP-based processes are preferable to those based on HPT. The results from solid-

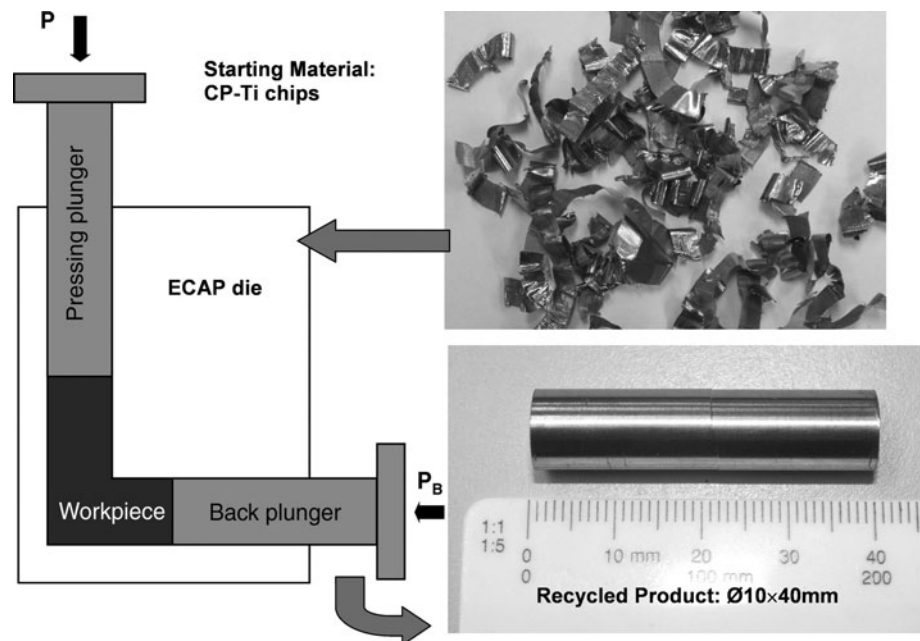
state recycling of commercially pure Ti machining chips using BP-ECAP will be reported, demonstrating its feasibility as a potential commercial process.

Experimental materials and procedures

Commercially pure (CP) Ti (ASTM grade 2) was used. Dry milling was employed to obtain the rectangular-shaped chips shown in Fig. 1 which also illustrates the solid-state recycling process by BP-ECAP. The BP-ECAP facility used is the same as that in, for example [18]. It has a 90° die with sharp corners and a round cross-section of 11 mm in diameter. A back plunger was used in the exit channel to provide a constant pressure of 50 MPa. The ECAP temperatures were 450 and 590 $^\circ\text{C}$, respectively, controlled to $\pm 1^\circ\text{C}$ through a thermocouple in contact with the die near the intersection of the channels. The as-received chips were wrapped in steel foil with graphite lubrication, and placed in the entrance channel before heating started. When the temperature stabilised, pressing started at a constant speed of 5 mm/min for 2, 4 and 8 passes, respectively, following route C, i.e. rotating the sample along its longitudinal axis by 180° between passes.

After consolidation, densities were measured based on the Archimedes principle. Samples for metallography were prepared by grinding and polishing following standard procedures, and etched in a solution of H_2O (100 mL), HF (3 mL) and HNO_3 (5 mL) to reveal grain boundaries. The grain sizes were measured following the procedures in ASTM standard E112-95. Samples for TEM (Tecnai-F20,

Fig. 1 Illustration showing the solid-state recycling process for Ti machining chips by back pressure equal channel angular pressing (BP-ECAP)



200 kV) observations were prepared using twin-jet electropolishing (Tenupol-3, Struer) with a solution containing H_2SO_4 (10%) in methanol at $-30\text{ }^\circ\text{C}$ and 20 V; further thinning was carried out using the Gatan precision ion polishing system (PIPS, model 691) with Ar-beam energy of 4 keV at an incident angle of $\pm 4^\circ$. Vickers microhardness was obtained on the polished specimen with a load of 0.1 kg for a holding time of 15 s. Compression tests at room temperature were conducted using samples of sizes $4 \times 4 \times 6\text{ mm}$ (with 6 mm as height along the longitudinal direction of the ECAP sample) to obtain the 0.2% proof stress. In addition, oxygen (O) and nitrogen (N) contents were analysed using a LECO TC600.

Experimental results and discussion

Microstructures

The contour of the as-received CP-Ti machining chips is shown in Fig. 2. According to Shankar et al. [19], the seemingly “featureless” chips under optical microscope consisted of a number of parallel slip bands in which shearing occurred, and within each band, the severe deformation would have resulted in substantial grain refinement leading to the formation of grains of the order of 100 nm in size. When the chips were compacted, a large amount of surface area existed, similar to the case in a powder compact. However, the oxide layer on the chips was likely to be thicker than that on particles because it formed at high temperatures during milling. The boundaries between the chips were thus comprised of oxide layers seen as thick dark lines from etching using optical microscopy. Figure 3 shows the morphology of these boundaries prior to and after

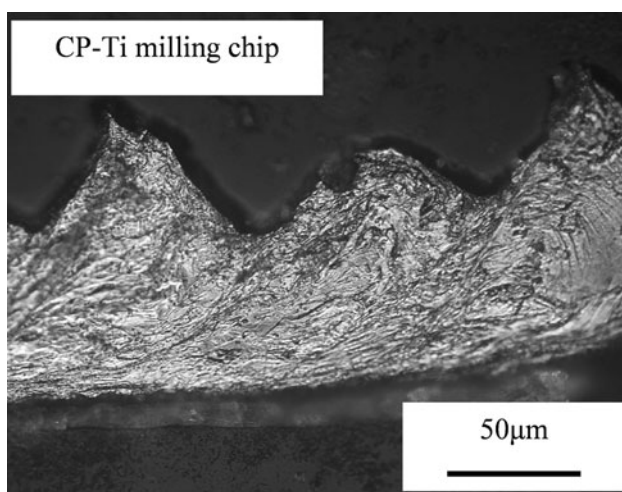


Fig. 2 Contour of an as-received Ti machining chip

the shearing deformation in ECAP at $450\text{ }^\circ\text{C}$. Before shearing, most chips were compressed to lie parallel to each other with boundaries perpendicular to the longitudinal direction of the sample in the entrance channel (Fig. 3a). After shearing under ideal conditions with sharp corners, the chips were deformed along the principal strain direction which lies 22.5° from the longitudinal direction of the sample in the exit channel, as calculated in [20]. This led to still parallel chip boundaries at approximately an angle of 22.5° (Fig. 3b). With multiple passes of ECAP following route C, after an even number of passes, the orientation of the chip boundaries should return to their original one (perpendicular to the longitudinal direction of the sample), as shown in Fig. 3c for a sample after 4 passes at $450\text{ }^\circ\text{C}$. However, after repeated shear deformation, the straightness and continuity of the boundary layer were disrupted with wavy and broken boundaries (Fig. 3c). It is expected that route B_c (i.e. rotating the sample by 90° in the same direction between passes) would be more effective in causing the fragmentation of the boundaries.

The ultrafine grains in the as-received chips were lost during the heating process prior to ECAP, growing to $\sim 5\text{--}10\text{ }\mu\text{m}$. Full consolidation was achieved in all the materials with densities from 4.50 to 4.53 g/cm^3 . In addition, grain refinement took place, as expected, during ECAP. The grain size versus number of passes is plotted in Fig. 4. The most significant reduction appeared to occur in the first two passes as dislocation multiplication and/or dynamic recrystallisation [21] were likely to dominate. In the subsequent passes, as plastic strain and exposure time at high temperatures increased, grains underwent slight growth [22, 23]. The refinement and coarsening would eventually reach an equilibrium with little coarsening from 8 to 16 passes at $590\text{ }^\circ\text{C}$ (Fig. 4). It is also obvious that the grains were finer at the lower processing temperature.

After ECAP for 8 passes at $590\text{ }^\circ\text{C}$, TEM observations showed mostly equiaxed grains with well-defined grain boundaries as well as subgrain boundaries and intragranular dislocations, as shown in Fig. 5. This is typical of the microstructure of a material which has undergone severe plastic deformation at high temperatures, displaying a balance between dislocation multiplication and dynamic recrystallisation.

Mechanical properties

The compressive true stress versus true strain curves for the CP-Ti materials recycled using BP-ECAP for 2 and 8 passes at 450 and $590\text{ }^\circ\text{C}$, respectively, are shown in Fig. 6. The average grain size, 0.2% proof stress and Vickers microhardness (HV) in different materials are displayed in Table 1. It can be seen that the 0.2% proof stress in the recycled materials increased significantly with a decrease

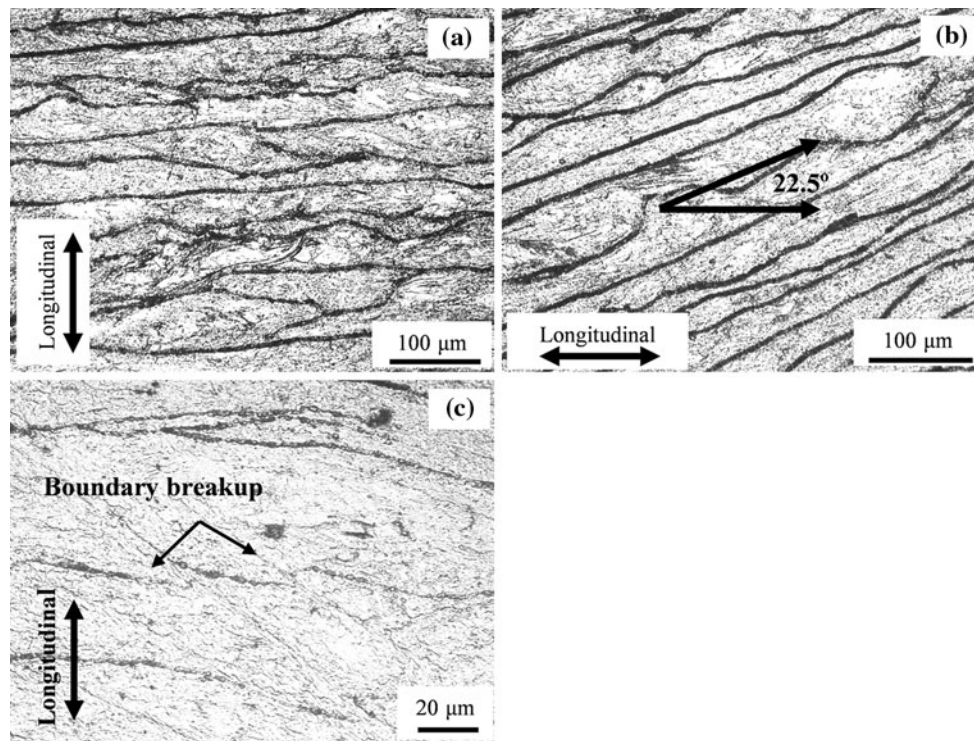


Fig. 3 Optical microstructures showing chip boundaries **a** prior to, and after shear deformation in ECAP at 450 °C for **b** one pass and **c** four passes

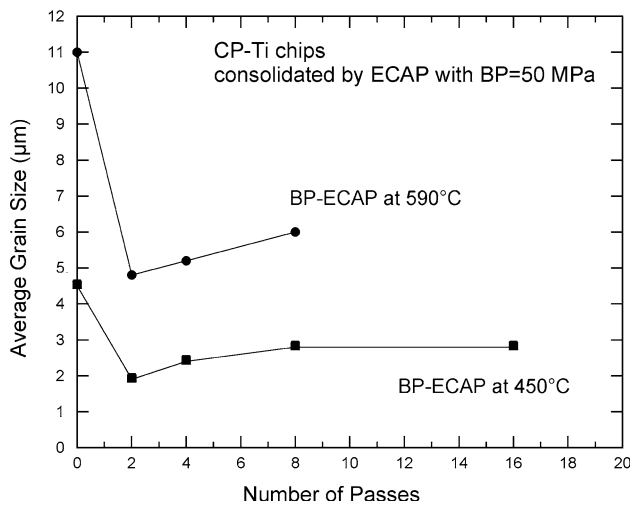


Fig. 4 Grain size as a function of the number of passes at 450 and 590 °C

in processing temperature from 590 to 450 °C. The 0.2% proof stress reached as high as 650 MPa when BP-ECAP was carried out at 450 °C for 2 passes, 220 MPa higher than 430 MPa achieved at 590 °C. These are significantly higher than those obtained in grade 2 CP-Ti rod (305 MPa) and sheet (340 MPa) after annealing. This is obviously due to the much finer grains in the ECAP processed materials. It is worth noting that the yield strength tends to decrease

with the number of passes after 2 passes (a decrease of 85 MPa from 2 to 8 passes at 450 °C, and 60 MPa at 590 °C). HV values demonstrate similar trends. This observation is consistent with the fact that grains coarsened slightly from 2 to 8 passes (Fig. 4). The 0.2% proof stress and HV are plotted against $d^{-1/2}$ (d is the grain size) in Fig. 7 for the materials listed in Table 1. It is apparent that the Hall–Petch relationship fits well in the forms of (d in m)

$$\sigma_{0.2} \text{ (MPa)} = \sigma_0 + K_y d^{-1/2} = 20.64 + 0.890 d^{-1/2} \quad (1)$$

$$H \text{ (MPa)} = H_0 + K_H d^{-1/2} = 1123.9 + 1.652 d^{-1/2} \quad (2)$$

where σ_0 (=20.64 MPa) and H_0 (=1123.9 MPa) are the lattice friction stress and hardness required to move individual dislocations, K_y (=0.890 MPa m^{1/2}) and K_H (=1.652 MPa m^{1/2}) the constants defining the slope of the lines in Fig. 7. It is thus clear that the variation in the yield strength can be largely explained by the difference in grain sizes.

It is of interest to compare the results with those obtained by others. Stolyarov et al. [24] investigated improving mechanical properties in bulk pure Ti by ECAP, and showed that the yield strength reached 640 MPa in a material with an average grain size of 0.28 μm after ECAP for 8 passes (1st pass at 450 °C and decreasing to 400 °C at the 8th pass) following route B_c. Similarly, in [25], ECAP (7 passes following route B_c with the 1st pass at 500 °C

Fig. 5 TEM microstructures in the sample after 8 passes at 590 °C, showing **a** mostly equiaxed grains, and **b** subgrain boundaries and dislocations at a higher magnification

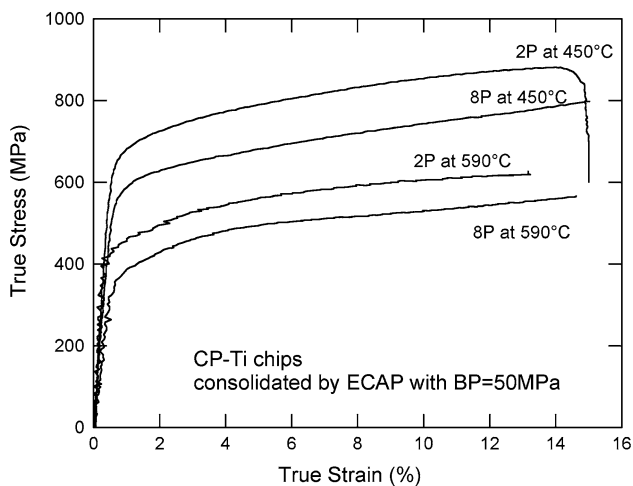
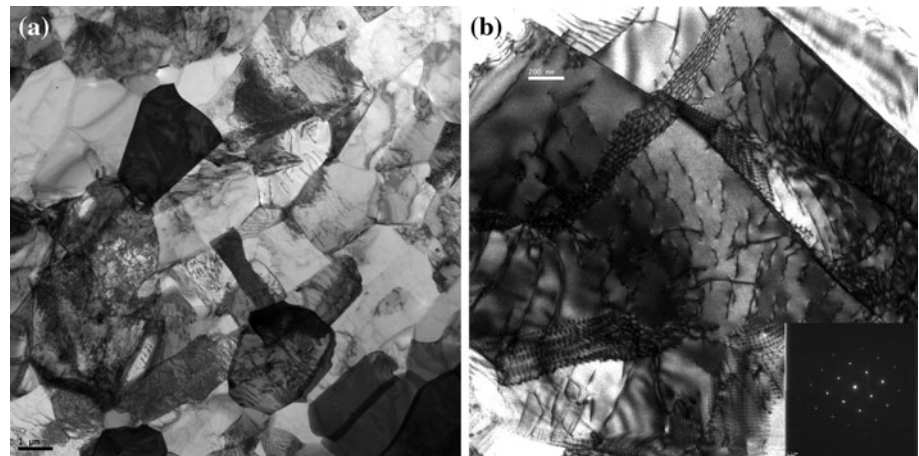


Fig. 6 Compressive true stress versus true strain curves for the Ti materials recycled using BP-ECAP for 2 and 8 passes at 450 and 590 °C, respectively

and last pass at 450 °C) was employed to achieve an average grain size of $\sim 0.3 \mu\text{m}$, resulting in yield strength of 520 MPa and HV of 2350 MPa. An yield strength of 630 MPa was also achieved in a pure Ti consolidated from particles by BP-ECAP for one pass at 600 °C [10]. It is thus obvious that the recycled Ti produced here by using BP-ECAP is as good as or better than those obtained by ECAP of ingot Ti or particulate Ti.

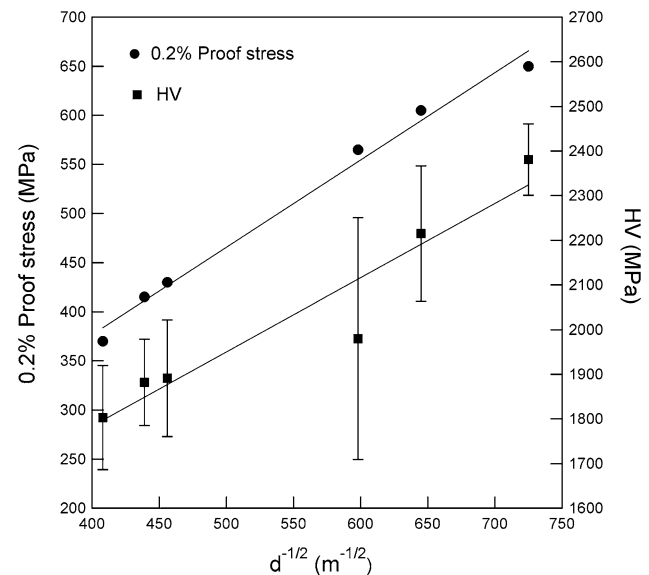


Fig. 7 The yield strength (0.2% proof stress) and Vickers microhardness (HV) versus $d^{-1/2}$ (d : grain size), showing the observation of the Hall–Petch relationship in the consolidated Ti

Effects of oxygen and surface oxide

Although grain refinement seems to be the dominant factor in the strengthening of the recycled Ti, other effects such as interstitial contents should be considered. The mechanical properties of Ti are sensitive to its interstitial contents, e.g. interstitial oxygen of 0.8 wt% or nitrogen of 0.4 wt% would

Table 1 Average grain sizes, HV values and 0.2% proof stresses of CP-Ti after ECAP consolidation at 450 and 590 °C for 2, 4 and 8 passes, respectively

	2 pass		4 pass		8 pass	
	450 °C	590 °C	450 °C	590 °C	450 °C	590 °C
Grain size (μm)	1.9	4.8	2.4	5.2	2.8	6.0
HV (MPa)	2381 \pm 80	1891 \pm 131	2215 \pm 152	1882 \pm 97	1980 \pm 271	1803 \pm 117
0.2% Proof stress (MPa)	650	430	605	415	565	370

lead to total embrittlement [26]. However, Xu et al. [10] demonstrated that BP-ECAP for 1 pass at 630 °C could improve plasticity in an ultrahigh strength (yield strength of 1350 MPa) Ti with high interstitial contents (1.34 wt% of oxygen and 0.3 wt% of nitrogen) consolidated from dehydrided particles. In the present work, the as-received CP-Ti chips possessed 0.20 wt% O and less than 0.01 wt% N, consistent with the specified composition of grade 2 Ti.

To estimate the respective contributions of interstitial oxygen and surface oxide to the total oxygen content analysed, it is useful to conduct the following calculation. First, a small number of the Ti chips was picked randomly and their mass (*m*) and surface area (*A*) were measured and calculated. Assuming the oxide is composed of the more stable TiO₂ rather than TiO with a thickness of *t*, the volume of the oxide layer is $V = A \cdot t$ and the mass of TiO₂ is $m_{\text{TiO}_2} = V \cdot \rho$, where, ρ is the density of TiO₂. In TiO₂, the weight percent of oxygen can be calculated as

$$\text{wt\% (O)} = \frac{16 \times 2}{47.9 + 16 \times 2} = 0.4005 \quad (3)$$

where 47.9 and 16 are the atomic weights of Ti and O, respectively. That is, oxygen accounts for 40.05% in weight in TiO₂. Thus, the mass of oxygen contained in the oxide layer is

$$m_{\text{oxygen in TiO}_2} = 0.4005m_{\text{TiO}_2} = 0.4005A \cdot t \cdot \rho \quad (4)$$

and the contribution of this oxygen to the total analysis is

$$\begin{aligned} \text{wt\% O (contributed by TiO}_2\text{)} &= \frac{m_{\text{oxygen in TiO}_2}}{m} \\ &= \frac{0.4005 \cdot A \cdot \rho \cdot t}{m} \cdot t \quad (5) \end{aligned}$$

Using the measured values of *m* and *A* as well as the density for TiO₂ (4.23 g/cm³) this linear relationship is plotted in Fig. 8. In the case of the as-received Ti chips, the analysed oxygen content is 0.2 wt%, the same as the specified composition for grade 2 Ti. Therefore, the thickness of the oxide layer must be very thin, perhaps less than 25 nm according to Fig. 8.

After ECAP consolidation at 450 °C, chemical analysis showed no increase in oxygen and nitrogen contents. At the higher processing temperature of 590 °C, the oxygen and nitrogen contents were increased to 0.3 and 0.02 wt%, respectively, i.e. slight increases were observed. It is likely that the increase in oxygen is due to oxidation (equivalent of ~100 nm thick oxide layer based on Fig. 8) rather than increased amount of interstitial oxygen. It can be concluded that interstitial oxygen and nitrogen played little role in strengthening in the recycled Ti, especially at the lower processing temperature of 450 °C.

On the other hand, oxygen may affect the mechanical properties in the form of surface oxide. The oxide might

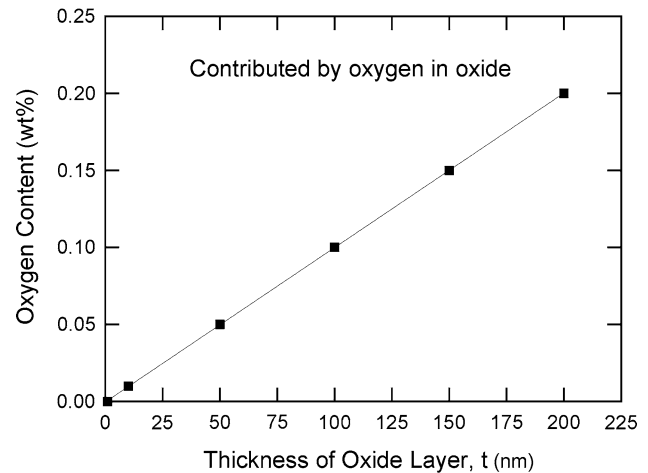


Fig. 8 Contribution to the total oxygen content from oxide as a function of the thickness of the surface oxide layer

provide dispersion strengthening as fine particles uniformly distributed in the matrix, or it could cause brittleness when a continuous network of oxide or large chunks is formed. Mabuchi et al. [13] employed hot extrusion to achieve a dispersion of oxide in the metal matrix, which was believed to be partly responsible for the enhanced mechanical properties of the recycled AZ91 Mg alloy. Oxide dispersion strengthening (ODS) was also reported by Chino et al. [14] in a recycled AZ31 Mg alloy by hot extrusion, and pure Fe through a combination of hot extrusion and annealing [27]. With the severe plastic deformation experienced in ECAP, there was indication that the original surface oxide layer on the machining chips could be broken with a large number of passes (Fig. 3c). However, route C is probably not the most effective. Further work is needed with a view to producing a fine dispersion of particles from these surface oxides so that it plays a positive role in strengthening.

Comparison with other solid-state recycling processes

What has been accomplished in this work demonstrates both scientific and technological significance of BP-ECAP in recycling waste in manufacturing by directly converting machining chips into fully dense bulk material with good mechanical properties and low energy consumption. The simplicity of BP-ECAP makes it a promising process to achieve value-adding solid-state recycling [28] compared to other conventional recycling technique such as hot extrusion and re-melting. An extremely high extrusion ratio of 1600:1 was used in order to recycle the AZ31 Mg alloy chips into bulk product with average grain size of 6.4 μm [14]. On the other hand, in order to recycle Ti–6Al–4V chips, an elaborate process was employed combining re-melting, forging and large strain hot-rolling [29]. By contrast, BP-ECAP only needs 2 passes to obtain a fully

dense fine-grained bulk material with good mechanical properties.

Summary and conclusions

- (1) Ti machining chips were successfully recycled using BP-ECAP, a solid-state process. Full density and good bonding were reached after only two passes at 450 or 590 °C.
- (2) The highest yield strength of 650 MPa was obtained in a material consolidated by BP-ECAP for two passes at 450 °C. In general, the yield strength and microhardness depend on grain size, following the well-known Hall–Petch relationship. The strength is comparable or better than those obtained from ECAP of either ingot or particulate Ti.
- (3) With repeated ECAP deformation, the surface oxide layer was gradually fragmented, potentially leading to additional dispersion strengthening and avoidance of adverse effects from continuous oxide network.
- (4) BP-ECAP is promising as a solid-state, value-adding recycling process especially for Ti machining chips which are highly reactive and account for a significant proportion of Ti manufacturing in such industries as aerospace and biomedical.

Acknowledgements This research was supported by the Defence Materials Technology Centre (DMTC). The authors gratefully acknowledge X. Wu, W. Xu, S. Goussous and E. W. C. Lui at the University of Melbourne for their assistance in BP-ECAP experiments and valuable discussions, and X. Yan at the Commonwealth Scientific and Industrial Research Organization (CSIRO) for his help in chemical analysis.

References

1. Gleiter H (2000) *Acta Mater* 48:1
2. Koch CC (2007) *J Mater Sci* 42:1403. doi:[10.1007/s10853-006-0609-3](https://doi.org/10.1007/s10853-006-0609-3)
3. Valiev RZ (2004) *Nature Mater* 3:511
4. Valiev RZ, Langdon TG (2006) *Prog Mater Sci* 51:881
5. Zhilyaev AP, Langdon TG (2008) *Prog Mater Sci* 53:893
6. Xia K (2008) *Mater Sci Forum* 579:61
7. Xia K (2010) *Adv Eng Mater* (in press)
8. Xu W, Honma T, Wu X, Ringer SP, Xia K (2007) *Appl Phys Lett* 91:031901
9. Xu W, Wu X, Honma T, Ringer SP, Xia K (2009) *Acta Mater* 57:4321
10. Xu W, Wu X, Sadedin D, Wellwood G, Xia K (2008) *Appl Phys Lett* 92:011924
11. Goussous S, Xu W, Wu X, Xia K (2009) *Comp Sci Technol* 69:1997
12. Murr LE, Quinones SA, Gaytan SM, Lopez MI, Rodela A, Martinez EY, Hernandez DH, Martinez E, Medina F, Wicker RB (2009) *J Mech Behavior Biomed Mater* 2:20
13. Mabuchi M, Kubota K, Higashi K (1995) *Mater Trans JIM* 36:1249
14. Chino Y, Hoshika T, Lee J-S (2006) *J Mater Res* 21:754
15. Lu L, Lai MO, Lim SH, Chua BW, Yan C, Ye L (2006) *Z Metall* 97:169
16. Peng T, Wang QD, Lin JB (2009) *Mater Sci Eng A516*:23
17. Lapovok R, Thomson PF (2004) In: Zehetbauer M, Valiev RZ (eds) *Nanomaterials by severe plastic deformation*. Wiley-VCH, Weinheim, Germany, p 551
18. Xia K, Wu X (2005) *Scripta Mater* 53:1225
19. Shankar MR, Rao BC, Lee S, Chandrasekar S, King AH, Compton WD (2006) *Acta Mater* 54:3691
20. Xia K, Wang J (2001) *Metall Mater Trans A* 32A:2639
21. Kim I, Kim J, Shin DH, Lee CS, Hwang SK (2003) *Mater Sci Eng A* 342:302
22. Zhu XJ, Tan MJ, Zhou W (2005) *Scripta Mater* 52:651
23. Tan MJ, Zhu XJ (2006) *J Achiev Mater Manuf Eng* 18:183
24. Stolyarov VV, Zhu YT, Alexandrov IV, Lowe TC, Valiev RZ (2003) *Mater Sci Eng A* 343:43
25. Stolyarov VV, Zhu YT, Lowe TC, Islamgaliev RK, Valiev RZ (1999) *NanoStruct Mater* 11:947
26. Conrad H (1981) *Prog Mater Sci* 26:123
27. Chino Y, Iwasaki H, Mabuchi M (2004) *J Mater Res* 19:1524
28. Aizawa T, Halada K, Gutowski TG (2002) *Mater Trans* 43:390
29. El-Morsy A-W (2009) *Mater Des* 30:1825